An Improved Multiband-Structured Subband Adaptive Filter Algorithm

Feiran Yang, Ming Wu, Peifeng Ji, and Jun Yang, *Senior Member, IEEE*

***Abstract*—Recently, a multiband-structured subband adaptive filter (MSAF) algorithm was proposed to speed up the convergence of the normalized least-mean-square (NLMS) algorithm. In this letter, we extend this work and propose an improved multiband-structured subband adaptive filter (IMSAF) algorithm to increase the convergence speed of the MSAF, which can also be regarded as a unifying framework for the NLMS, MSAF, and affine projection (AP) algorithms. The proposed optimization criterion is based on the principle of minimal disturbance, canceling the most recent P *a posteriori* errors in each of the N subbands. The stability condition and the computational complexity are also analyzed. Computer simulations in the context of system identification demonstrate the effectiveness of the new algorithm.**

***Index Terms*—Acoustic echo cancellation, convergence rate, subband adaptive filter, subband update.**

I. Introduction

ADAPTIVE filtering plays an important role in many signal processing applications such as adaptive beamforming, channel equalization, and acoustic echo cancellation (AEC). The normalized least-mean-square (NLMS) algorithm is widely used due to its simplicity and robust performance. However, the NLMS algorithm has slow convergence with colored input signals [1]. Therefore, the subband adaptive filter (SAF) [1] has been proposed to improve the convergence behavior of the NLMS algorithm. The conventional subband structure achieves some reduction in the computational complexity and increases the convergence rate. However, its convergence speed is still limited due to aliasing and band-edge effects [1], [2].

To solve this problem, Lee and Gan [3] presented a multiband-structured subband adaptive filter (MSAF)[1] algorithm to accelerate the convergence rate for input signals having a large spectral dynamic range. The MSAF algorithm updates the fullband tap weights of the modeling filter using subband signals normalized by their respective subband input variance. The MSAF algorithm has recently been the subject of intensive investigation [1], [3]–[7].

Some applications such as AEC involve colored signals, and hence require high-order filters to model long acoustic impulse response. In such cases the convergence rate of the MSAF algorithm needs to be improved. In this letter, we will extend the work in [3] and propose an improved MSAF (IMSAF) algorithm to speed up the convergence. The MSAF algorithm is derived based on the principle of minimal disturbance by nulling the current N subband errors. Data-reuse algorithms are considered an alternative to increase the convergence speed by recycling the old data signal, e.g., the affine projection (AP) algorithm [8]. Inspired by this idea, a new optimization criterion is proposed based on the principle of minimal disturbance by canceling the most recent P *a posteriori* errors in each of the N subbands, i.e., a total of PN error signals instead of N for the MSAF algorithm. The new algorithm is derived using the method of Lagrange multipliers. The stability condition and the computational load are analyzed. Moreover, it is shown that the IMSAF algorithm can be viewed as a generalized form of the NLMS, MSAF, and AP algorithms. The performance is then evaluated via computer simulation in the context of system identification.

Throughout this letter, vectors and matrices will be denoted by boldface symbols, $(\cdot)^T$ denotes the transpose operator, $\|\cdot\|^2$ represents squared Euclidean norm of a vector, and $E(\cdot)$ takes expectation.

II. Review of the MSAF Algorithm

Consider the desired response $d(n)$ that arises from the linear model

$$d(n) = \mathbf{w}_{\mathrm{o}}^T \mathbf{u}(n) + v(n) \tag{1}$$

where $\mathbf{w}_{\mathrm{o}} = [w_0, w_1, \ldots, w_{L-1}]^T$ is the length-L tap-weight vector of the unknown system, $\mathbf{u}(n) = [u(n), u(n-1), \ldots, u(n-L+1)]^T$ denotes the input signal vector, and $v(n)$ represents the system noise.

Fig. 1 shows a block diagram of the MSAF. The desired signal $d(n)$ and input signal $u(n)$ are partitioned into N subband signals, $d_i(n)$ and $u_i(n)$, by means of analysis filters $H_i(z)$. The subband input signals $u_i(n)$ are filtered by the adaptive filter to generate the subband output signals $y_i(n)$. The subband signals $d_i(n)$ and $y_i(n)$ are then decimated by a factor N to generate $d_{i,\mathrm{D}}(k)$ and $y_{i,\mathrm{D}}(k)$. We use $F_i(z)$ to denote the synthesis filter. The notations $\downarrow N$ and $\uparrow N$ represent N-fold decimation and interpolation. Variables n and k are used to indicate the original and decimated sequences. The *a priori* and *a posterior* decimated subband errors are defined as, respectively,

$$e_{i,\mathrm{D}}(k) = d_{i,\mathrm{D}}(k) - \mathbf{w}^T(k)\mathbf{u}_i(k), \tag{2}$$

$$\xi_{i,\mathrm{D}}(k) = d_{i,\mathrm{D}}(k) - \mathbf{w}^T(k+1)\mathbf{u}_i(k) \tag{3}$$

Manuscript received May 24, 2012; revised June 28, 2012; accepted July 19, 2012. Date of publication July 24, 2012; date of current version August 08, 2012. This work was supported by National Natural Science Fund of China under Grants 11004217, 11074279, and 11174317. The associate editor coordinating the review of this manuscript and approving it for publication was Prof. Saeed Gazor.

The authors are with the State Key Laboratory of Acoustics and the Key Laboratory of Noise and Vibration Research, Institute of Acoustics, Chinese Academy of Sciences, Beijing 100190, China (e-mail: feirany.ioa@gmail.com; mingwu@mail.ioa.ac.cn; jipeifeng@mail.ioa.ac.cn; junyang.ioa@gmail.com).

Color versions of one or more of the figures in this paper are available online at http://ieeexplore.ieee.org.

Digital Object Identifier 10.1109/LSP.2012.2210213

[1]As one of the reviewers pointed out, it was named "normalized SAF" in [3]. To highlight the multiband nature, it was called "MSAF" in [1].

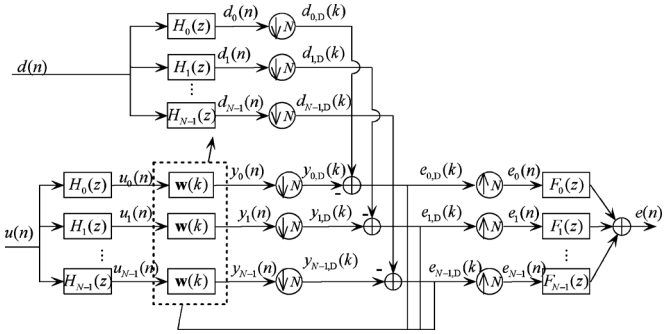

Fig. 1. Block Diagram of the MSAF.

where

$$\mathbf{u}_i(k) = [u_i(kN), u_i(kN-1), \ldots, u_i(kN-M+1)]^T$$

denotes the regression vector for the ith subband signal and $\mathbf{w}(k) = [w_0(k), w_1(k), \ldots, w_{M-1}(k)]^T$ is the weight vector of the fullband adaptive filter. We use M to denote the length of the modeling filter.

The MSAF can be obtained based on the principle of minimal disturbance by canceling the *a posteriori* errors in all N subbands at each iteration k, i.e.,

$$\min_{\mathbf{w}(k+1)} \|\mathbf{w}(k+1) - \mathbf{w}(k)\|^2 \quad \text{subject to } \xi_{i,\mathrm{D}}(k) = 0, i = 0, 1, \ldots, N-1. \quad (4)$$

The weight vector $\mathbf{w}(k)$ is adapted as follows [1]:

$$\mathbf{w}(k+1) = \mathbf{w}(k) + \mu \sum_{i=0}^{N-1} \frac{\mathbf{u}_i(k)}{\|\mathbf{u}_i(k)\|^2 + \alpha} e_{i,\mathrm{D}}(k) \quad (5)$$

where μ is the step size and α is a small positive constant to avoid possible division by zeros.

III. Proposed IMSAF Algorithm

A. Derivation of the IMSAF Algorithm

From (4) we know the MSAF algorithm is obtained by minimizing the squared Euclidean norm of the change in the tap-weight vector subject to the set of N constraints imposed on the decimated filter output. Motivated by the AP algorithm, we might utilize additional recent data to update the adaptive filter. We propose to cancel the most recent P *a posteriori* errors in each of the N subbands, i.e., a total of PN error signals instead of N as in the MSAF algorithm, and then obtain

$$d_{i,\mathrm{D}}(k-j) = \mathbf{w}^T(k+1)\mathbf{u}_i(k-j), \quad i = 0, 1, \ldots, N-1; j = 0, 1, \ldots, P-1. \quad (6)$$

In order to obtain a compact solution, we define the following quantities:

$$\begin{aligned}\mathbf{U}(k) = [&\mathbf{u}_0(k), \ldots, \mathbf{u}_0(k-P+1), \mathbf{u}_1(k), \\ &\ldots, \mathbf{u}_1(k-P+1), \\ &\ldots, \mathbf{u}_{N-1}(k), \ldots, \mathbf{u}_{N-1}(k-P+1)], \quad (7)\\ \mathbf{d}_{\mathrm{D}}(k) = [&d_{0,\mathrm{D}}(k), \ldots, d_{0,\mathrm{D}}(k-P+1), d_{1,\mathrm{D}}(k), \\ &\ldots, d_{1,\mathrm{D}}(k-P+1), \ldots, d_{N-1,\mathrm{D}}(k), \\ &\ldots, d_{N-1,\mathrm{D}}(k-P+1)]^T, \quad (8)\end{aligned}$$

$$\begin{aligned}\mathbf{e}_{\mathrm{D}}(k) = [&e_{0,\mathrm{D}}(k), \ldots, e_{0,\mathrm{D}}(k-P+1), e_{1,\mathrm{D}}(k), \\ &\ldots, e_{1,\mathrm{D}}(k-P+1), \ldots, e_{N-1,\mathrm{D}}(k), \\ &\ldots, e_{N-1,\mathrm{D}}(k-P+1)]^T \\ = &\mathbf{d}_{\mathrm{D}}(k) - \mathbf{U}^T(k)\mathbf{w}(k), \quad (9)\\ \boldsymbol{\xi}_{\mathrm{D}}(k) = [&\xi_{0,\mathrm{D}}(k), \ldots, \xi_{0,\mathrm{D}}(k-P+1), \xi_{1,\mathrm{D}}(k), \\ &\ldots, \xi_{1,\mathrm{D}}(k-P+1), \ldots, \xi_{N-1,\mathrm{D}}(k), \\ &\ldots, \xi_{N-1,\mathrm{D}}(k-P+1)]^T \\ = &\mathbf{d}_{\mathrm{D}}(k) - \mathbf{U}^T(k)\mathbf{w}(k+1), \quad (10)\\ \mathbf{v}_{\mathrm{D}}(k) = [&v_{0,\mathrm{D}}(k), \ldots, v_{0,\mathrm{D}}(k-P+1), v_{1,\mathrm{D}}(k), \\ &\ldots, v_{1,\mathrm{D}}(k-P+1), \ldots, v_{N-1,\mathrm{D}}(k), \\ &\ldots, v_{N-1,\mathrm{D}}(k-P+1)]^T \\ = &\mathbf{d}_{\mathrm{D}}(k) - \mathbf{U}^T(k)\mathbf{w}_{\mathrm{o}} \quad (11)\end{aligned}$$

where P is the projection order. The constraint conditions in (6) are now expressed more compactly as

$$\mathbf{U}^T(k)\mathbf{w}(k+1) = \mathbf{d}_{\mathrm{D}}(k). \quad (12)$$

We now seek $\mathbf{w}(k+1)$ by solving the constrained optimization criterion:

$$\min_{\mathbf{w}(k+1)} \|\mathbf{w}(k+1) - \mathbf{w}(k)\|^2 \quad \text{subject to} \quad \boldsymbol{\xi}_{\mathrm{D}}(k) = \mathbf{0} \quad (13)$$

where $\mathbf{0}$ is the $NP \times 1$ null matrix. The constrain minimization problem can be solved by the method of Lagrange multipliers. We choose the cost function as:

$$J[\mathbf{w}(k+1)] = \frac{1}{2}\|\mathbf{w}(k+1) - \mathbf{w}(k)\|^2 + \boldsymbol{\lambda}^T \boldsymbol{\xi}_{\mathrm{D}}(k) \quad (14)$$

where $\boldsymbol{\lambda} = [\lambda_0, \lambda_1, \ldots, \lambda_{NP-1}]^T$ is the Lagrange multipliers vector pertaining to the constrains in (12). Taking the derivative of (14) with respect to $\mathbf{w}(k+1)$ and setting it to zero, we obtain

$$\mathbf{w}(k+1) = \mathbf{w}(k) + \mathbf{U}(k)\boldsymbol{\lambda}. \quad (15)$$

Substituting (15) into (12) and using (9), one has

$$\mathbf{U}^T(k)\mathbf{U}(k)\boldsymbol{\lambda} = \mathbf{e}_{\mathrm{D}}(k). \quad (16)$$

Solving $\boldsymbol{\lambda}$ from (16) and substituting it into (15), we obtain a recursive relation for updating the tap-weight vector:

$$\mathbf{w}(k+1) = \mathbf{w}(k) + \mu\mathbf{U}(k)\left[\mathbf{U}^T(k)\mathbf{U}(k)\right]^{-1}\mathbf{e}_{\mathrm{D}}(k). \quad (17)$$

To avoid potential numerical instability, a regularization parameter ε is added to the diagonal elements of $\mathbf{U}^T(k)\mathbf{U}(k)$. Therefore a more practical update equation of the IMSAF algorithm becomes

$$\mathbf{w}(k+1) = \mathbf{w}(k) + \mu\mathbf{U}(k)\left[\mathbf{U}^T(k)\mathbf{U}(k) + \varepsilon\mathbf{I}\right]^{-1}\mathbf{e}_{\mathrm{D}}(k) \quad (18)$$

where $\mathbf{I}$ is the identity matrix with size $NP \times NP$. The weight update of the IMSAF is similar to that of the AP algorithm; the only difference is that the matrix $\mathbf{U}(k)$ of the AP algorithm is composed of the fullband signal vectors, whereas that of the IMSAF algorithm consists of the subband signal vectors. If the off-diagonal elements of $\mathbf{U}^T(k)\mathbf{U}(k)$ are negligible, (18) can also be simplified to the form of (5). The cross-correlation items

$\mathbf{u}_i^T(m)\mathbf{u}_p(m-l)$ of two arbitrary subband signals may be neglected by a properly designed analysis filter. However, the autocorrelation elements $\mathbf{u}_i^T(m)\mathbf{u}_i(m-l)$ can not be ignored because the correlation in subbands is also high for highly colored signals. As a result, the off-diagonal elements of $\mathbf{U}^T(k)\mathbf{U}(k)$ can not be ignored.

We define $\mathbf{U}^{(l)}$ as the lth column vector of $\mathbf{U}(k)$ and $\mathbf{d}_{\mathrm{D}}^{(l)}$ as the lth element of $\mathbf{d}_{\mathrm{D}}(k)$. Equivalently, the solution of (13) can also be expressed as [9], [10]:

$$\mathbf{w}(k+1) = \mathbf{w}(k) + \sum_{l=0}^{NP-1} \frac{\mu \mathbf{x}^{(l)} e^{(l)}}{\left\|\mathbf{x}^{(l)}\right\|^2} \tag{19}$$

where $\mathbf{x}^{(0)} = \mathbf{U}^{(0)}$, and $\mathbf{x}^{(m)}$ is the component of $\mathbf{U}^{(m)}$ that is orthogonal to $\mathbf{U}^{(0)}, \mathbf{U}^{(1)}, \ldots, \mathbf{U}^{(m-1)}$, and

$$\begin{aligned} e^{(0)} &= \mathbf{d}_{\mathrm{D}}^{(0)} - \mathbf{w}^T(k)\mathbf{U}^{(0)}, \\ e^{(m)} &= \mathbf{d}_{\mathrm{D}}^{(m)} - \left(\mathbf{w}^{(m)}\right)^T \mathbf{U}^{(m)}, m = 1, \ldots, NP-1, \\ \mathbf{w}^{(m)} &= \mathbf{w}(k) + \sum_{l=0}^{m-1} \frac{\mu \mathbf{x}^{(l)} e^{(l)}}{\left\|\mathbf{x}^{(l)}\right\|^2}. \end{aligned} \tag{20}$$

When the input signal is highly colored, the successive input vectors tend to be almost parallel to each other, so the weight estimate improves little during successive iteration [9]. From (20), it is noted that the proposed algorithm carries out an orthogonalization procedure to the successive input vectors and, therefore, speeds up the convergence.

B. Relationship to Other Adaptive Filters

In the special case $P = 1$, only the current N subband data are used to update the weight vector and (13) reduces to (4), so the IMSAF algorithm reduces to the MSAF algorithm. In the special case $N = 1$, the filter bank reduces to a single filter with its impulse response given by the unit impulse $\delta(n)$ and the signal reconstruction is not required [4]. Furthermore, (13) becomes the optimization criterion used in the derivation of the AP algorithm, so the IMSAF algorithm reduces to the AP algorithm. And in the special case where both $P = 1$ and $N = 1$, the IMSAF algorithm reduces to the NLMS algorithm. Thus, the IMSAF algorithm can be considered as a generalized form of the NLMS, AP, and MSAF algorithms.

The IMSAF algorithm generalizes the MSAF along the time axis using multiple time-domain constraints, generalizes the AP along the frequency axis using multiple subband constraints, and generalizes the NLMS along both the frequency axis, using multiple subband constraints, and the time axis, using multiple time-domain constraints. In other words, compared with NLMS, the AP algorithm improves the convergence rate by data-reuse, the MSAF algorithm speeds up the convergence by subband decomposition that whitens the input signal, and the IMSAF algorithm speeds up the convergence by both data-reuse and subband decomposition.

C. Stability of the IMSAF Algorithm

We assume the adaptive filter has the same order as the real system. The mismatch between $\mathbf{w}_{\mathrm{o}}$ and $\mathbf{w}(k)$ is measured by the tap-weight error vector $\mathbf{f}(k) \equiv \mathbf{w}_{\mathrm{o}} - \mathbf{w}(k)$. Using (17), we obtain

$$\mathbf{f}(k+1) = \mathbf{f}(k) - \mu \mathbf{U}(k)\left[\mathbf{U}^T(k)\mathbf{U}(k)\right]^{-1}\mathbf{e}_{\mathrm{D}}(k). \tag{21}$$

A stability analysis is carried out based on the mean-square deviation (MSD). Taking the expectation of the squared norm on both sides of (21), we obtain:

$$\begin{aligned} \delta_f^2(k+1) = \delta_f^2(k) &+ \mu^2 E\left\{\mathbf{e}_{\mathrm{D}}^T(k)\left[\mathbf{U}^T(k)\mathbf{U}(k)\right]^{-1}\mathbf{e}_{\mathrm{D}}(k)\right\} \\ &- 2\mu E\left\{\mathbf{f}^T(k)\mathbf{U}(k)\left[\mathbf{U}^T(k)\mathbf{U}(k)\right]^{-1}\mathbf{e}_{\mathrm{D}}(k)\right\} \end{aligned} \tag{22}$$

where $\delta_f^2(k) \equiv E\left\{\|\mathbf{f}(k)\|^2\right\}$. Using (9) and (11), the subband error signal vector $\mathbf{e}_{\mathrm{D}}(k)$ can be expressed as

$$\mathbf{e}_{\mathrm{D}}(k) = \mathbf{e}_P(k) + \mathbf{v}_{\mathrm{D}}(k) \tag{23}$$

where $\mathbf{e}_P(k) = \mathbf{U}^T(k)\mathbf{f}(k)$ is the modeling error vector. Substituting into (22) yields

$$\begin{aligned} \delta_f^2(k+1) = \delta_f^2(k) &+ \mu^2 E\left\{\mathbf{e}_{\mathrm{D}}^T(k)\left[\mathbf{U}^T(k)\mathbf{U}(k)\right]^{-1}\mathbf{e}_{\mathrm{D}}(k)\right\} \\ &- 2\mu E\left\{\mathbf{e}_P^T(k)\left[\mathbf{U}^T(k)\mathbf{U}(k)\right]^{-1}\mathbf{e}_{\mathrm{D}}(k)\right\}. \end{aligned} \tag{24}$$

In order to obtain monotonic convergence and stability, the MSD $\delta_f^2(k)$ must decrease with increasing k, i.e., $\delta_f^2(k+1) < \delta_f^2(k)$. Thus the step size is bounded as

$$0 < \mu < 2\frac{E\left\{\mathbf{e}_P(k)\left[\mathbf{U}^T(k)\mathbf{U}(k)\right]^{-1}\mathbf{e}_{\mathrm{D}}(k)\right\}}{E\left\{\mathbf{e}_{\mathrm{D}}^T(k)[\mathbf{U}^T(k)\mathbf{U}(k)]^{-1}\mathbf{e}_{\mathrm{D}}(k)\right\}}. \tag{25}$$

Denoting $\Theta(k) = \delta_f^2(k) - \delta_f^2(k+1)$, if we choose μ such that $\Theta(k)$ is maximized, the fastest convergence rate is obtained because the MSD undergoes the largest decrease from iteration k to iteration $k+1$. Then the optimal step size satisfies $\partial\Theta(k)/\partial\mu = 0$, and solving yields

$$\mu_{\mathrm{opt}} = \frac{E\left\{\mathbf{e}_P(k)\left[\mathbf{U}^T(k)\mathbf{U}(k)\right]^{-1}\mathbf{e}_{\mathrm{D}}(k)\right\}}{E\left\{\mathbf{e}_{\mathrm{D}}^T(k)[\mathbf{U}^T(k)\mathbf{U}(k)]^{-1}\mathbf{e}_{\mathrm{D}}(k)\right\}}. \tag{26}$$

In the absence of disturbance, we obtain $\mathbf{e}_{\mathrm{D}}(k) = \mathbf{e}_P(k)$ from (23). Thus, the condition on the step-size parameter $0 < \mu < 2$ ensures the adaptive filter convergence in the mean-square sense, and it is clear from (26) that the algorithm achieves the fastest convergence rate for $\mu_{\mathrm{opt}} = 1.0$.

D. Computational Complexity

We now analyze the computational complexity of the IMSAF algorithm. It should be noted that the tap-weight vector is adapted every N samples, compared to every sample for the fullband case. It is assumed that the cost of inverting a $P \times P$ matrix is $O(P^3)$ operations [11]. Calculation of $\mathbf{U}^T(k)\mathbf{U}(k)$ requires $2PN^3$ multiplications using a recursive approach. The IMSAF algorithm requires a total of $2PM + P(2N^2 + 1) + O(N^2P^3) + L(N+2)$ multiplications during a single sampling period T_{s}, compared to $2PM + 3P + O(P^3)$ for the AP algorithm [12] and $3M + 2 + L(N+2)$ for the MSAF algorithm [1]. Similar to the AP algorithm, the improvement of convergence rate for the IMSAF algorithm is at the cost of increased computational complexity. However, it is possible to reduce the computational complexity significantly based on dichotomous coordinate descent (DCD) iterations [12].

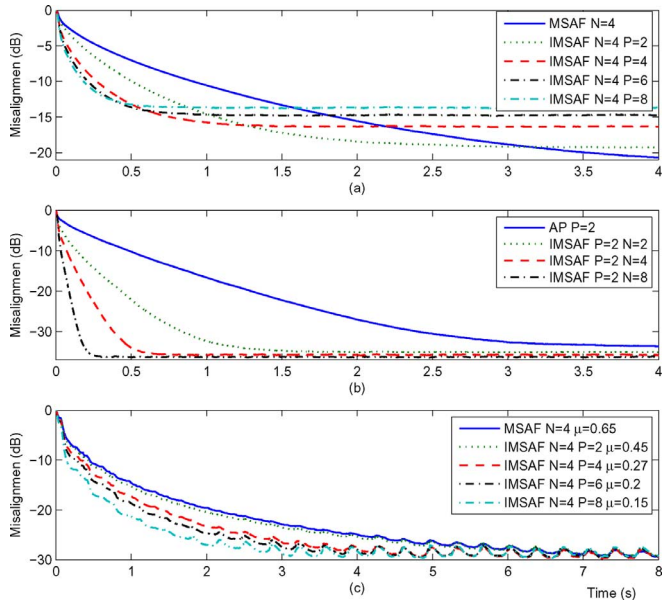

Fig. 2. Convergence characteristics of the IMSAF algorithm. (a) Learning curves for the IMSAF and MSAF. $\mu = 1.0$, $M = L = 512$, $N = 4$, $\mathrm{SNR} = 30$ dB, AR(10) input signal. (b) Learning curves for the IMSAF and AP. $\mu = 1.0$, $L = 256$, $M = 230$, $P = 2$, AR(10) input signal. (c) Learning curves for the IMSAF and MSAF. $M = L = 1024$, $N = 4$, $\mathrm{SNR} = 30$ dB, CCS input.

IV. Simulation Results

The simulation is carried out in the context of system identification. The impulse response $\mathbf{w}_o$ is generated according to $w_i = e^{-\tau i} r(i)$, $i = 0, 1, \ldots, L-1$, where $r(i)$ is a zero-mean white noise sequence and τ is the envelope decay rate. The sampling rate is 8 kHz. The input signals are an AR(10) process [1] and the composite source signal (CCS) specified by the ITU G.168 standard. Cosine modulated filter banks are used for the subband structure. The convergence performance is evaluated in terms of the normalized misalignment (in dB) defined as $10\log_{10}\left[\|\mathbf{w}_o - \mathbf{w}(k)\|^2 / \|\mathbf{w}_o\|^2\right]$. For AR(10) input, the results are obtained by averaging over 100 Monte Carlo trials.

In the first set of simulations, the convergence rate of the IMSAF algorithm is compared to that of the MSAF with the AR(10) signal. The length of the adaptive tap-weight vector is $M = L = 512$. An independent white Gaussian noise signal is added to the echo signal, with 30-dB signal-to-noise ratio (SNR). The projection orders of the IMSAF are $P = 2$, 4, 6, and 8. The number of subband is $N = 4$. We choose $\mu = 1.0$ for all cases to obtain the fastest convergence. From the learning curves in Fig. 2(a), it is clear that the IMSAF algorithm provides faster convergence than the MSAF algorithm for the same number of subband. It is also noted that larger P leads to faster convergence speed but also higher steady-state misadjustment. This is mainly because nulling PN *a posteriori* errors will force the adaptive filter to compensate for the effect of a noise signal that is uncorrelated with the input signal [13]. We also note that increasing P from 6 to 8 does not significantly improve the convergence speed.

In the second set of simulations, the convergence behavior of the IMSAF is investigated for the AR(10) signal in a noise-free environment, where the length of the real system is $L = 256$ and the order of the adaptive filter is $M = 230$. The unmodeled tail of the response forms a disturbance to the system. The projection order of the IMSAF and AP is 2. The subband number of the IMSAF is set to $N = 2$, 4, and 8. From Fig. 2(b), it can be noted that the IMSAF algorithm exhibits faster convergence than the AP algorithm. For the IMSAF, the convergence performance improves as the number of subbands increase.

In the third set of simulations, we evaluate the performance of the proposed algorithm with CCS input. CCS has properties similar to those of speech with voiced and unvoiced segments as well as pauses. We use $M = L = 1024$, $N = 4$, and $\mathrm{SNR} = 30$ dB. The projection orders of the IMSAF are $P = 2$, 4, 6, and 8. Step sizes are chosen such that identical steady-state misadjustment is achieved for all cases. As can be seen from Fig. 2(c), the IMSAF algorithm also achieves good results for a highly non-stationary signal in a noisy environment.

V. Conclusion

In this letter, we have proposed an improved version of the MSAF algorithm based on nulling additional *a posteriori* errors in each subband. By increasing the projection order and/or number of subbands, the proposed IMSAF algorithm achieves faster convergence speed with highly correlated signals. We also show that the IMSAF algorithm is a generalization of several other known adaptive filtering algorithms. Simulation results verify the validity and performance advantage of the new algorithm.

References

[1] K. A. Lee, W. S. Gan, and S. M. Kuo, *Subband Adaptive Filtering: Theory and Implementation*. Chichester, U.K.: Wiley, 2009.
[2] D. R. Morgan, "Slow asymptotic convergence of LMS acoustic echo cancelers," *IEEE Trans. Speech Audio Process.*, vol. 3, no. 2, pp. 126–136, Mar. 1995.
[3] K. A. Lee and W. S. Gan, "Improving convergence of the NLMS algorithm using constrained subband updates," *IEEE Signal Process. Lett.*, vol. 11, no. 9, pp. 736–739, Sep. 2004.
[4] K. A. Lee and W. S. Gan, "Inherent decorrelating and least perturbation properties of the normalized subband adaptive filter," *IEEE Trans. Signal Process.*, vol. 54, no. 11, pp. 4475–4480, Nov. 2006.
[5] J. Ni and F. Li, "A variable regularization matrix normalized subband adaptive filter," *IEEE Signal Process. Lett.*, vol. 16, no. 2, pp. 105–108, Feb. 2009.
[6] J. Ni and F. Li, "A variable step-size matrix normalized subband adaptive filter," *IEEE Trans. Audio, Speech Lang. Process.*, vol. 18, no. 6, pp. 1290–1299, Aug. 2010.
[7] W. Yin and A. S. Mehr, "Stochastic analysis of the normalized subband adaptive filter algorithm," *IEEE Trans. Circuits Syst. I*, vol. 58, no. 5, pp. 1020–1033, May 2011.
[8] K. Ozeki and T. Umeda, "An adaptive filtering algorithm using an orthogonal projection to an affine subspace and its properties," *Electron. Commun. Jpn.*, vol. 67-A, no. 5, pp. 19–27, May 1984.
[9] S. G. Sankaran and A. A. L. Beex, "Normalized LMS algorithm with orthogonal correction factors,yr," in *Proc. Thirty-First Asilomar Conf. Signals, Syst., Comput.*, Pacific Grove, CA, Nov. 1997, pp. 2–5.
[10] S. G. Sankaran and A. A. L. Beex, "Convergence behavior of affine projection algorithms," *IEEE Trans. Signal Process.*, vol. 48, no. 4, pp. 1086–1096, Apr. 2000.
[11] A. H. Sayed, *Adaptive Filters*. New York: Wiley, 2008.
[12] Y. Zakharov, "Low complexity implementation of the affine projection algorithm," *IEEE Signal Processing Lett.*, vol. 15, pp. 557–560, 2008.
[13] M. Rupp, "A family of adaptive filter algorithms with decorrelating properties," *IEEE Trans. Signal Process.*, vol. 46, no. 3, pp. 771–775, Mar. 1998.